RESOURCE SAVINGS IN GRIDLESS COHERENT SUBMARINE NETWORKS WITH FILTERLESS ARCHITECTURES

Md. Nooruzzaman, Feriel Nabet, Nabih Alloune, Émile Archambault, Christine Tremblay (École de technologie supérieure, Canada),
Marija Furdek, Jiajia Chen, Lena Wosinska (KTH Royal Institute of Technology, Sweden),
Paul Littlewood and Michel P. Bélanger (Ciena Corporation, Canada)
Email: christine.tremblay@etsmtl.ca

École de technologie supérieure, 1100 Notre-Dame West, Montréal, QC, H3C 1K3, Canada

Abstract: Flexible and scalable networking solutions are required to offer more efficient bandwidth allocation and increased connectivity in submarine networks. In this regard, filterless optical networks based on agile edge nodes equipped with coherent transceivers and passive broadcast-and-select nodes are promising cost-effective options which allow for more flexible capacity allocation and resource optimization in the optical layer. In this paper, we evaluate possible resource and cost savings in a filterless submarine network architecture.

1. INTRODUCTION

A new generation of high-capacity optical networks has been enabled by coherent detection and digital signal processing (DSP) technologies. Coherent optical transmission systems operating at 100 Gb/s are currently deployed over ultra-long distances for both terrestrial and transoceanic applications [1, 2].

As the global traffic increases and becomes more dynamic, the need for agile networking solutions becomes more and more important for optimizing the network resources. In terrestrial networks, the agility is obtained by equipping the nodes with active photonic switching components such as reconfigurable optical add-drop multiplexers (ROADMs) based on wavelength selective switch (WSS) technologies. In today's submarine networks, WSS-based ROADMs can be deployed at the cable landing stations (the dry plant) [3, 4]. However, the branching units (BUs) deployed in the wet plant for connecting the branches to the trunk of undersea networks include passive or power-switched fiber joints or fixed OADMs. They employ a fixed, pre-determined wavelength arrangement and are not flexible in terms of connectivity, which limits the network reconfiguration and spectrum reassignment capability of current undersea networks.

Due to the harsh deployment environment and the constraints of system repair, submarine transmission systems are expected to exhibit high reliability and a 25-year operating lifetime. This puts stringent limitations on the technology and qualification requirements for the components and subsystems that can be deployed in the wet plant [4]. Reconfigurable BUs based on passive multiplexer/demultiplexer (mux/demux), wavelength blocker (WB) and WSS technologies have been proposed recently [5, 6]. Submarine ROADMs using passive optical interleavers and de-interleavers have also been proposed [6]. However, these devices have limited reconfiguration capability and still require several qualification tests (in terms of performance, robustness, lifetime and packaging) before they can be deployed under sea.

A filterless network architecture based on passive broadcast-and-select nodes and DSP-assisted coherent transceivers at the edge nodes has been proposed recently for introducing agility in submarine networks [3]. In this paper, a filterless architecture for a long haul (LH) submarine optical network is presented and resource savings are shown through comparative spectrum consumption and cost analysis with a conventional solution.

2. FILTERLESS SUBMARINE NETWORKS

Fig. 1 illustrates the architecture of a typical 6-node LH submarine network with a conventional trunk and branch architecture [3]. A 3-fiber-pair optical line system is deployed in the 8,000-km main trunk between nodes 1 and 6, and 4 BUs are used for connecting nodes 2 to 5 to the main trunk. The black FP provides the basic connectivity between the 6 nodes. The green and blue FPs would be typically used to carry the express traffic between specific nodes, as well as to provide protection against failure by rerouting traffic on an alternative FP. Trunk and branch submarine networks are typically based on 2 to 4 fiber pairs (FPs); therefore, this 3-FP architecture can be considered as a realistic deployment case. In this example, the BUs are composed of passive fiber joints, providing a fixed connectivity between specific sets of terrestrial nodes.

Fig. 2 shows the proposed filterless solution for the LH submarine network. The nodal architecture of the cable landing stations is shown in Fig. 3 for both the conventional and filterless solutions. In the filterless architecture, the WSS and mux/demux devices deployed at the submarine line terminal equipment (SLTE) are replaced by passive splitters and combiners, leading to a significant cost reduction. Erbium-doped fiber amplifiers

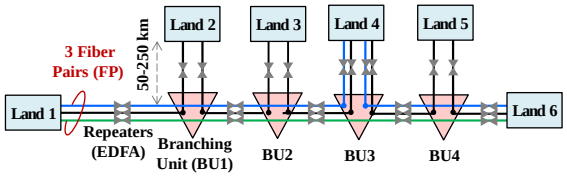

Figure 1: Conventional architecture for a 6-node LH submarine network. Land: cable landing station.

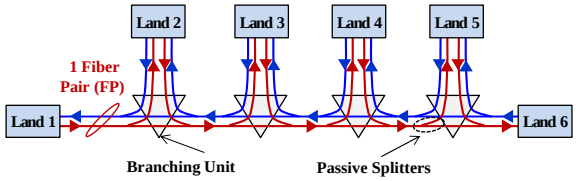

Figure 2: Filterless architecture for a 6-node LH submarine network.

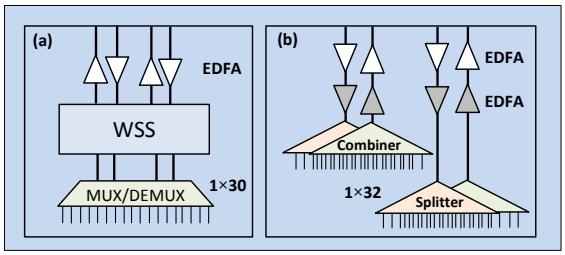

Figure 3: (a) Conventional and (b) filterless node architecture.

(EDFAs) are used for compensating the extra component loss.

The filterless solution, which requires only a 1-FP cable line system in the trunk for providing connectivity among all nodes, can accommodate up to 16 Tb/s of traffic (80 x 100G wavelength channels in each direction) [3]. This may reduce the initial installation investment.

In the filterless network architecture, network reconfigurability is provided by coherent transceivers equipped with DSP modules for chromatic dispersion (CD), polarization mode dispersion (PMD) and forward error correction (FEC). Dual-polarization quadrature phase shift keying (DP-QPSK) or dual-carrier binary phase shift keying (DP-BPSK) channels can be used at 100 Gb/s to achieve the distances required in transoceanic submarine applications. The wavelength channels are broadcasted from the source nodes to a plurality of nodes through passive splitters and combiners that are already qualified

for submarine applications and the destination nodes select the desired channels from the received optical signal by tuning the local oscillator of the coherent receivers. In such a scheme, the channel wavelength (and/or bandwidth) can be adjusted through software control of the coherent transponders, which allows for a flexible assignment of the spectrum according to the traffic changes and ensures fast resource optimization through elastic networking.

3. ENABLING FLEXIBILITY WITH ELASTIC FILTERLESS OPTICAL NETWORKING

The passive gridless architecture of filterless networks makes them suitable for elastic optical networking, which can improve flexibility and spectrum utilization. Namely, the gridless operation can be achieved and the spectrum granularity can be decreased at almost no cost without having to deploy gridless ROADMs which are currently more expensive than fixed-grid ones.

Fig. 4 illustrates the spectrum utilization flexibility allowed by programmable coherent transponders in which the modulation format and corresponding channel capacity can be selected on a per channel basis to best match the capacity-reach to be implemented. Moreover, this flexibility permits to accommodate deployed channels using more advanced modems occupying larger spectrum.

Several of the advantages allowed by a gridless operation are illustrated in Fig. 4. The inherent flexibility of the filterless architecture allows for reassigning the installed capacity to adjust to variations of traffic in a transoceanic system crossing several time zones. In long transoceanic systems, time-varying traffic at different nodes reaches peak and trough values at different times during the day. Without

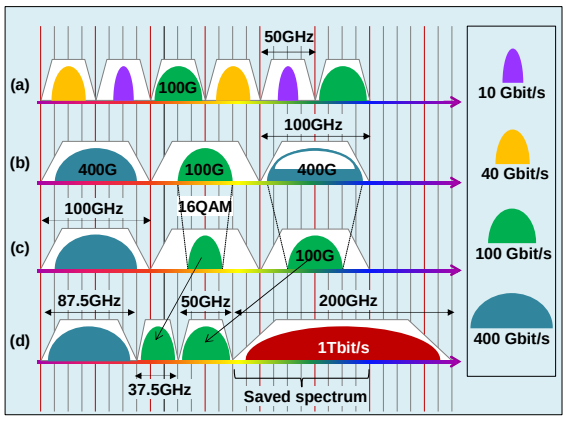

Figure 4: Spectral saving enabled by elastic networking [7]: (a) a 50-GHz grid has a maximum capacity of 100 Gb/s per DP-QPSK channel; (b) a 100-GHz grid has a maximum capacity of 400 Gb/s per DP-QPSK or 16-quadrature amplitude modulation (QAM) channel; (c) multirate channel deployment on a fixed grid; (d) multirate channel deployment on a flexible grid. Assumptions: 12.5-GHz frequency slot unit (FSU) and guard band.

flexibility, the transceivers used at a given node might be subject to a broadly varying fill factor and thus exhibit widely variable cost effectiveness. By dynamically adjusting the number of transceivers and wavelengths between the nodes so as to match the traffic variations, network resources can be used more efficiently.

Fig. 5 shows an example of wavelength reconfiguration in a filterless architecture. Let us assume nodes 2 and 3 experience the peak load at two different periods t_1 and t_2, respectively. A single transceiver (i.e., Tx3) connects node 1 to nodes 2 and 3, respectively, at two different times t_1 and t_2 using the same wavelength, i.e., λ_3.

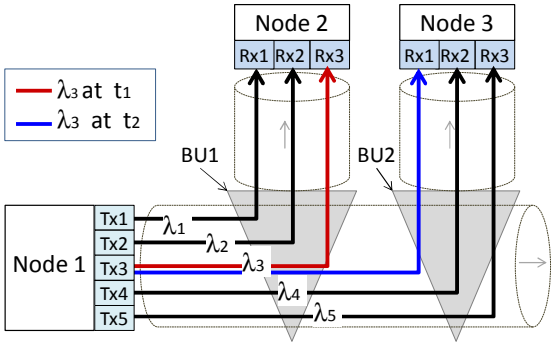

Figure 5: Example of wavelength reconfiguration in a filterless network. Note that for simplicity only one direction of the signals is shown.

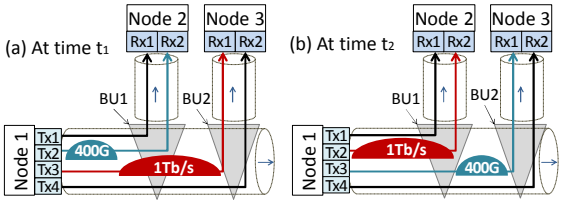

Figure 6: Example of spectrum reconfiguration in a filterless network.

Similarly, Fig. 6 illustrates how spectrum reconfiguration can be realized in a filterless network.

4. CAPACITY ANALYSIS

Fig. 7 shows the capacity limits of both the conventional and filterless solutions. The wavelength consumption was evaluated as a function of the total network traffic volume. The capacity limit is defined as the total traffic supported by the network when at least one of the fibers is fully loaded. The channel characteristics are shown in Table 1. The reach and capacity constraints were set to 8,000 km and 80 wavelengths, which can be considered good assumptions for a 100G DP-QPSK transmission system deployed over a low-loss (0.16 dB/km) cable line system with no inline CD compensation [8].

The initial traffic matrix (expressed in 100G units) is non-uniform and includes a total of 58 demands [3]. The traffic evolution relates to the populations of source node p_i and destination node p_j, and their respective traffic growth rates g_i and g_j as follows:

$$d_{ij}^{n} = d_{ij}^{n-1} \times \left\{1 + (P_i \times g_i + P_j \times g_j)/(P_i + P_j)\right\} \quad (1)$$

where d_{ij}^{n} is the traffic of n^{th} period between two cable landing stations i and j.

For the conventional solution, two cases were considered. In the first scheme, dedicated FPs are used to carry the traffic between specific node pairs, which corresponds to the realistic case where the 3 FPs would be used by different network operators. In the second (load balancing) scheme, all the traffic demands are first routed based on the shortest path, and then the demands on the congested paths are rerouted to the less loaded available fibers at the expense of an increased latency.

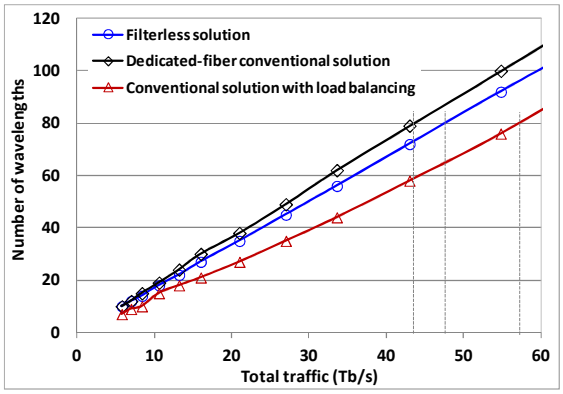

Figure 7: Wavelength consumption of fixed-grid conventional and filterless solutions.

Solution type	Channel capacity (Gb/s)	Modulation format	Spectral occupancy (GHz)	Reach (km)
Fixed-grid	100	DP-QPSK	50 GHz	8,000
Elastic	n×100	DP-QPSK	(n×3+1) ×12.5 GHz	8,000

Table 1: Fixed and flexible grid channel characteristics. Here, *n* is a positive integer.

Fig. 7 shows that the filterless solution can accommodate more traffic than the conventional "dedicated fiber" solution. From the results presented in Fig. 7, it can be concluded that the capacity limit of the filterless solution is approximately 8% higher than that of a conventional "dedicated fiber" solution and 16% lower than that of a conventional solution with load balancing.

The spectrum consumption, as well as the improvement in spectrum utilization, that can be achieved by using an elastic filterless approach instead of a conventional fixed-grid approach has been quantified as a function of the traffic load. The spectrum utilization improvement is defined as the ratio of the difference in spectrum usage between the elastic and fixed-grid cases over the spectrum consumed in the fixed-grid case. We compare two scenarios. In the "with

defragmentation" case, the total spectrum resources are reassigned in each traffic period. In the "without defragmentation" case, the spectrum assigned in previous traffic periods is not reassigned during the following periods.

Fig. 8a shows the spectrum consumption as a function of the traffic load in both fixed-grid and elastic filterless solutions compared to the fixed-grid conventional solution. The consumed spectrum is expressed in the number of frequency slot units (FSUs), where each FSU corresponds to 12.5 GHz. In the fixed-grid solutions, 50-GHz channels are considered. Therefore, a 500-Gb/s demand consumes 250 GHz of spectrum (5 × 50 GHz). On the other hand, in the flex-grid (elastic) solutions, a 37.5-GHz channel bandwidth per DP-QPSK channel is assumed. Therefore a 500-Gb/s demand requires a total bandwidth of 200 GHz (5 × 37.5 GHz + 12.5 GHz of guard band). This squeezes channels much closer together, without guard band between adjacent 100G channels of the same super-channel increasing the overall spectral efficiency.

The results show that elastic filterless solution exhibit a significant reduction in terms of spectrum consumption (up to about 30% in the "with defragmentation" case) at high traffic load, compared to the fixed-grid filterless solutions.

Fig. 8b shows the spectrum utilization improvement (SUI) of the fixed-grid and elastic filterless solutions with respect to the fixed-grid conventional solution as a function of the traffic. The SUI for the fixed-grid and the elastic filterless solutions was calculated by using equations (2) and (3), respectively:

$$SUI(\%) = 100 \times (\lambda^{con} - \lambda^{fil}) / \lambda^{con} \quad (2)$$

$$SUI(\%) = 100 \times (\lambda^{con} - \lambda^{fil}_{elas}) / \lambda^{con} \quad (3)$$

where λ^{con} is the spectrum consumed by fixed-grid conventional solution, and λ^{fil} and λ^{fil}_{elas} are the spectrum consumed by the fixed-grid and elastic filterless solutions, respectively. Note that λ^{fil}_{elas} in eq. (3) has two values: one for "with defragmentation" and the other one for "without defragmentation".

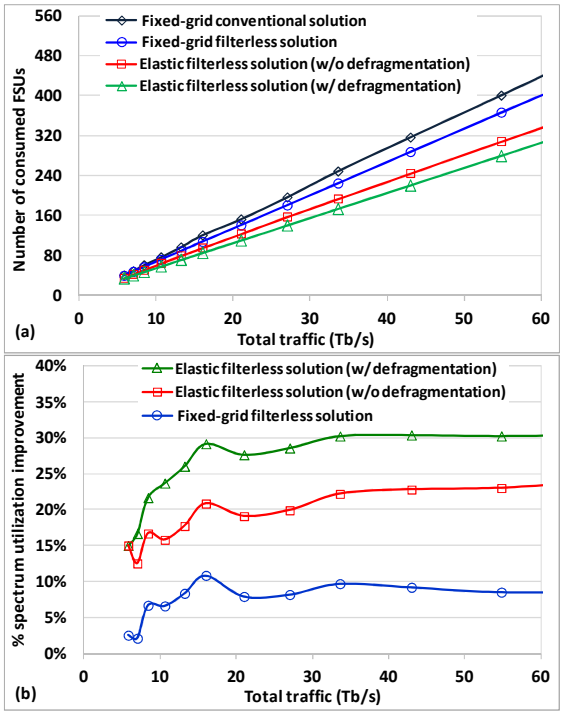

Figure 8: (a) Spectrum consumption and (b) spectrum utilization improvement achieved in the filterless solution with respect to the fixed-grid conventional solution as a function of traffic volume.

The results in Fig. 8b show that the fixed-grid filterless solution can achieve approximately 8% improvement in spectrum utilization on average over all traffic periods. Furthermore, more than 20% improvement in spectrum utilization can be achieved by using elastic filterless architecture for high traffic loads with no defragmentation, while defragmentation allows for about 30% spectrum savings. These results indicate that a significant amount of spectrum is freed up in an elastic filterless network, which can be used to add more channels in submarine networks. Inherently, the agility enabled by the filterless architecture translates into a higher capacity submarine cable.

5. COST ANALYSIS

A comparative cost analysis of filterless and conventional network solutions was performed. The cost assumptions for the terminal (SLTE) and line system equipment are listed in Table 2. The cost of the cable line system and the cost of the repeaters depend on the number of FPs, as well as on the type of cable (i.e., deep sea, continental shelf or armored). The installed first cost (IFC) of the filterless solution was calculated by assuming one 2-FP cable line system (which was assumed to be the minimum cable size) in the trunk and two 2-FP cable line systems in the branches. In the conventional solution, a 3-FP cable line system was assumed to be installed at the initial deployment.

The cost evolution of the terminal equipment for both filterless and conventional solutions as a function of traffic is shown in Fig. 9a. A comparison of IFC shows 27% cost saving in terminal equipment for the filterless solution as a result of the passive node architecture of the filterless nodes.

The cost evolution of the optical line system for both the filterless and conventional solutions is shown in Fig. 9b. A comparison of the IFC shows 11% cost saving in line system equipment for the filterless solution. A second 2-FP cable line system must be installed for the filterless solution when the total traffic reaches 33.6 Tb/s. For the conventional solutions, an additional 3-FP cable line system must be deployed when the total traffic reaches 54.8 Tb/s in the dedicated-fiber case and 70.2 Tb/s in the load balancing case.

	Extra components	Unit cost (a.u.)
SLTE	WSS	1.25
	1×30 Mux	0.31
	1×32 Splitter	0.16
	EDFA	0.62
Cable line system	2/3/4-FP Cable (deep sea, continental shelf, armored)	(0.9, 1.1, 2.3) / (1.0, 1.2, 2.5) / (1.1, 1.3, 2.7)
	2/3/4-FP Repeater	60/70/80

Table 2: Cost assumptions [3]. The unit costs of terminal and line system equipment are normalized to the cost of a 100G DP-QPSK modem and to the cost of a 3-FP deep-sea cable line system, respectively.

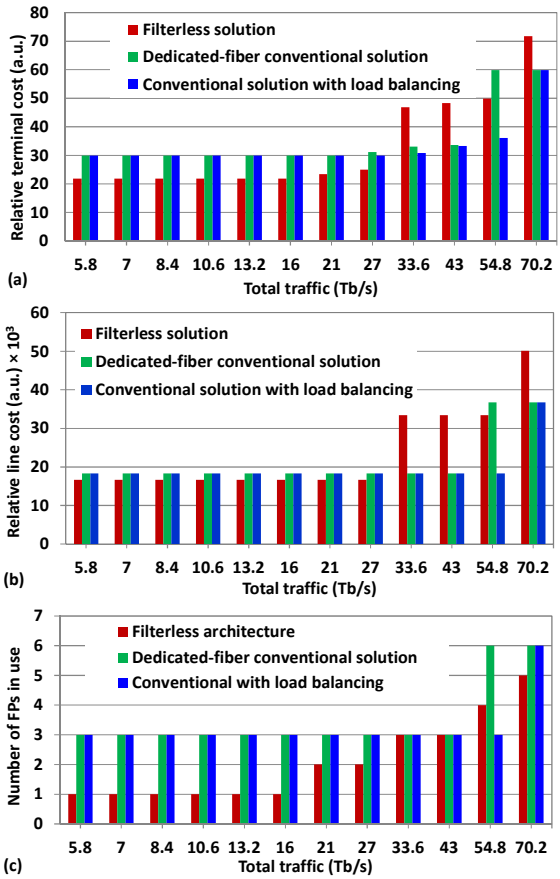

Figure 9: Cost evolution of filterless and conventional solutions as a function of traffic: (a) terminal costs; (b) line costs; (c) number of fiber pairs.

Fig. 9c shows the number of FPs used in the filterless and conventional solutions as the traffic increases. At the initial deployment, two FPs were considered in the cost calculations of the filterless solution (although only one FP is sufficient to support up to 16 Tb/s of traffic), which allows for a pay-as-you-grow scheme which is more flexible than the conventional solution.

6. CONCLUSIONS

In this paper, filterless and conventional solutions for a 6-node LH submarine

network topology are compared through a capacity and cost analysis. The results show that the capacity limit of the proposed filterless solution is approximately 8% higher compared to the conventional 3-FP solution. Thanks to the gridless feature of the filterless architecture, a 20% improvement in spectrum utilization is obtained by flexible spectrum assignment. A comparative cost analysis shows 27% and 11% cost saving in terminal and line equipment at initial deployment. Based on these results, gridless filterless architectures can be expected to bring in significant resource savings in submarine applications.

7. REFERENCES

[1] K. Roberts et al., "High Capacity Transport—100G and Beyond," J. Light. Technol., vol.33, no.3, pp.563-578, Feb.1, 1 2015.

[2] M. Salsi et al., "100 Gb/s and Beyond for Submarine Systems," J. Light. Technol., vol. 30, no. 24, pp. 3880-3887, 2012.

[3] M. Nooruzzaman et al., "Filterless architecture for coherent undersea networks," ONDM 2015, pp. 68-73, May 2015.

[4] S. Shapiro, "The Guide Session 2 – Network Design", SubOptic 2013, Paris, France, April 2013.

[5] Philip N. Ji et al., “Reconfigurable branching unit for submarine optical communication networks”, US Patent No. 20130259055 A1, October 2013.

[6] Philip N. Ji et al., “Submarine reconfigurable optical add/drop multiplexer with passive branching unit”, Patent No. US 2015/0043920 A1, February 12, 2015.

[7] O. Gerstel et al., "Elastic optical networking: a new dawn for the optical layer?," IEEE Commun. Mag., vol. 50, no. 2, pp. s12-s20, February 2012.

[8] J.-X. Cai at al., "Transmission of 96×100-Gb/s bandwidth-constrained PDM-RZ-QPSK channels with 300% spectral efficiency over 10,610 km and 400% spectral efficiency over 4,370 km," J. Light. Technol., vol. 29, no. 4, pp. 491- 498, 2011.

